Chemical screening pipeline for identification of specific plant autophagy modulators

Dauphinee AN[1†], Cardoso C[1,2†], Dalman K[1], Ohlsson JA[1], Berglund Fick S[3], Robert S[4], Hicks GR[5], Bozhkov PV[1], Minina EA[1,6*]

[1]Department of Molecular Sciences, Uppsala BioCenter, Swedish University of Agricultural Sciences and Linnean Center for Plant Biology, P.O. Box 7015, Uppsala, SE-750 07, Sweden

[2]Plant Genetics, School of Life Science Weihenstephan, Technical University of Munich (TUM), 85354 Freising, Germany

[3]Chemical Biology Consortium Sweden, Umeå University, 901 87 Umeå, Sweden

[4]Department of Forest Genetics and Plant Physiology, Umeå Plant Science Centre, Swedish University of Agricultural Sciences, 901 83 Umeå, Sweden.

[5]UCenter for Plant Cell Biology, University of California Riverside, 92521 California, USA

[6]COS, Heidelberg University. Im Neuenheimer Feld 230. 69120 Heidelberg, German

[†]These authors contributed equally to the work

*corresponding author

Abstract

Autophagy is a major catabolic process in eukaryotes and is implicated in responses to biotic and abiotic stresses, programs of aging and cell death. Autophagy is known to regulate agriculturally important traits such as plant fitness, longevity, biomass and seed yield. However, despite its obvious significance, there is still a shortage of reliable tools modulating plant autophagy. Here we describe the first robust pipeline for identification of specific plant autophagy-modulating compounds. Our novel screening protocol comprises four phases: (i) high-throughput screening of chemical compounds in cell cultures of *Nicotiana tabacum*; (ii) confirmation of the identified hits *in planta* using *Arabidopsis thaliana*; (iii) further characterization of the effect using conventional molecular biology methods; (iv) verification of specificity of the effect to autophagy *in planta*. The methods detailed here streamline identification of specific plant autophagy modulators and greatly aid in unravelling the molecular mechanisms of plant autophagy.

Main

Autophagy is a key regulator of eukaryotic cellular homeostasis and plays an essential role in abiotic and biotic stress responses, fecundity, aging and cell death[1–5]. The autophagy pathway comprises selective or bulk sequestration of cytosolic contents into double-membraned vesicles known as autophagosomes and their delivery to the lytic compartment, where autophagy activity (or autophagic flux) completes with the degradation of the delivered cargo[6]. Autophagy in eukaryotes is coordinated by evolutionary conserved autophagy-related (ATG) proteins that orchestrate sequestration of the cargo, formation and trafficking of the autophagosomes and cargo degradation. Among these proteins, ATG8 is remarkable in the sense that it is incorporated into the membranes of forming autophagosomes, trafficked to the lytic compartment and degraded together with the cargo, making it an ideal tool for autophagy activity read-out[7].

The importance of autophagy for plant stress tolerance in general and crop performance in particular is of critical interest in plant biology, requiring continuous development of increasingly sophisticated tools for its investigation[1,8]. The forward and reverse genetic approaches such as knockouts, knockdowns and overexpression of *ATG* genes, although being effective tools, have certain limitations[1,7]. The chemical modulation of autophagy presents an alternative option and has also been instrumental for our current understanding of the

underlying mechanisms controlling autophagy[7]. However, an increasing number of studies describe significant off-target effects of commonly used autophagy-modulating drugs. For example, 3-methyladenine (3-MA) that is typically used as an inhibitor of autophagy[7], can also increase autophagic flux after prolonged treatments due to its transient suppression of class III phosphoinositide 3-kinases (PI3Ks)[9]. Another autophagy inhibitor, chloroquine, has been recently shown to induce autophagy-independent severe disorganization of the Golgi and endo-lysosomal systems[10]. An enhancer of autophagy, rapamycin, extensively used for yeast and animal model systems is known to specifically form a ternary complex with the FKBP12 (12-kDa cis-trans peptidyl-prolyl isomerase FK506 Binding Protein) and the TOR (Target of Rapamycin) kinase[7,11] to induce autophagy. Nevertheless, an opposite effect is caused by high concentrations of rapamycin[12]. Furthermore, although rapamycin was originally thought to be ineffective in *Arabidopsis thaliana*[13], potentially due to the low capacity of plant FKB12 proteins to form the complex, a more recent report suggests this is not the case[14]. These studies illustrate the importance and need for better screening strategies to identify novel autophagy modulators. Furthermore, novel modulators of autophagy may play a critical role in understanding the underlying mechanisms regulating the process.

Here we describe the first robust pipeline for identification of chemical compounds specifically modulating plant autophagy. The assays utilize a combination of reporter and control transgenic lines to optimize the treatment conditions cell cultures and *in planta* and ensure that the compounds influence autophagic flux without causing considerable stress to other endomembrane compartments. Using this new method, we have identified several promising autophagy-modulating compounds.

Results

Screen overview

The pipeline comprises a combination of assays that have incremental decrease in throughput capacity, but increase in data depth and reliability (Fig. 1a). The assays are grouped into four phases, each providing a new level of information about investigated compounds. The combination of all phases, including the optimization of the upstream steps based on downstream results (see feedback connections in Fig. 1a) was optimized to provide reliable characterization of the compound effect *in vivo*.

Phase one – hit identification

78 The first phase was performed in the high-throughput mode using tobacco (*Nicotiana tabacum*
79 *L.* cv Bright Yellow 2) cell cultures[15] expressing chemiluminescent reporters for autophagic
80 flux (Fig. 1b). Transgenic BY-2 cells were incubated and treated in 96-well format, lysed in
81 the same plate and used for quantitative measurement of luminescence. In this assay the
82 reporter line was co-expressing *Renilla* luciferase (Rluc) fused to nuclear localization signal
83 (NLS) and firefly luciferase (Fluc) fused to ATG8. Upon activation of autophagy, Fluc-ATG8
84 was delivered to the lytic vacuole, where Fluc luminescence was quenched by the low pH,
85 resulting in increase of the ratio of Rluc/Fluc. In the control line both luciferases are targeted
86 to the nuclei, where they are protected from sequestration into autophagosomes. The dual
87 luciferase assay permits measurement of both response (Fluc: Fluc-ATG8 for the reporter line
88 and Fluc-NLS for the control line) and reference (Rluc-NLS) luminescence in the same cells,
89 thus removing possible bias originating from cell-to-cell expression level fluctuations or
90 differences in cell number per sample. Additionally, absolute values of the Rluc luminescence
91 can be used as a crude estimation of cell viability, as it generally dramatically decreases in
92 lysates of dying cells.

93 The growth and treatment conditions were preliminarily optimized using known inducers and
94 inhibitors of autophagy, e.g. AZD8055[16], benzothiadiazole (BTH)[17], concanamycin A[18]
95 (Supplementary Fig. 1a, b). Importantly, data from the viability assay of the phase two provided
96 a critical insight into an average range of compounds concentrations that are not toxic for BY-
97 2 cells (Fig. 2a). Thus it might be advisable to perform a screen of a relatively small number
98 of compounds first to estimate the optimal average concentration range for the library of
99 interest (feedback connection i, Fig. 1a). As a proof of concept, a set of 364 small organic
100 compounds of the PMRA[19] and PMRP[20] libraries was screened in this study and a total of 19
101 enhancers and 5 inhibitors of autophagy were chosen for further testing (Supplementary Fig.
102 1b).

103 **Phase two – hit optimization**

104 To enhance efficiency of the screen and promote an early elimination of compounds that do
105 not reveal *in vivo* activity, *in planta* assays were performed already at the second phase of the
106 screen.

107 Solubility assay. The first estimation of the applicable concentration range for the compounds
108 selected in phase one was performed by assessing their solubility in the media used for growing

109 cell cultures and seedlings at under the corresponding growth conditions. For each selected
110 compound we tested the concentration used in the first phase and additional concentrations that
111 were several-fold greater. Additionally, at this stage it is advisable to at least theoretically
112 predict the stability of the selected compounds under the treatment conditions[21]. This will allow
113 correct handling of the compounds based on factors such as sensitivity to aqueous solutions,
114 light or pH during upcoming experiments and omitting highly unstable compounds.

115 Viability assay. After estimating the range of possible concentrations determined by physical
116 characteristic of a compound it is essential to identify the maximal concentration that is not
117 cytotoxic. Each compound at its maximal concentration selected based on the results of the
118 solubility assay and also several serial dilutions were used for treatment of BY-2 cell cultures
119 and *Arabidopsis thaliana* seedlings. Viability of the plant material was assessed by
120 phenotyping specimens at 0-24 h of the treatment using differential interference contrast (DIC)
121 microscopy. Only the concentrations not causing any visible changes in cell morphology were
122 considered for further assays.

123 An example presented in Fig. 2 illustrates the dose-dependent toxicity of the compound 12
124 (C12) after a 4 h treatment. At 50 µM, C12 had no observable effect on the BY-2 cells (Fig.
125 2a), whereas the 200 µM treatment caused swelling of the cells (white arrows, Fig. 2a) and 400
126 µM C12 led to protoplast collapse (black arrows, Fig. 2a). Interestingly, we observed that on
127 average, root cells of Arabidopsis seedlings were considerably more sensitive to the drug
128 treatment than BY-2 cells (Fig. 2). For instance, a 100 µM treatment of C12 caused
129 condensation of cytoplasm in the epidermal root cells of Arabidopsis seedlings (white arrows,
130 Fig. 2b), whereas 200 µM C12 led to protoplast collapse (black arrows, Fig. 2b). The difference
131 in the sensitivity of the model system to the same compounds is an important factor to be
132 assessed for phase one optimization (feedback arrow i, Fig. 1a).

133 Tandem tag assay.

134 The first phase provides high-throughput quantitative data about delivery rate of the ATG8
135 fusion to the lytic compartment upon drug treatment of plant cell culture. Although this readout
136 usually well correlates with autophagy activity, it still might provide false positive and false
137 negative results. The Tandem Tag (TT) assay not only allows to assess time and dose-
138 dependent delivery rate of the ATG8 fusion to the lytic compartment upon drug treatment *in*
139 *planta*, but also yields important morphological data on autophagosome formation and

140 confirms that the observed changes in the ATG8 localization are autophagy-dependent. For
141 this assay, ATG8 fused to the fluorescent tandem tag consisting of TagRFP and mWasabi[12]
142 was expressed in the wild-type (WT) and autophagy-deficient Arabidopsis plants (reporter and
143 control lines for autophagic flux detection, respectively; Fig. 1c). Due to relatively high
144 stability of TagRFP fluorescence at the low pH of the lytic vacuole and poor low pH-tolerance
145 of mWasabi fluorescence, the ratio of the red to green fluorescence intensities in the vacuoles
146 can be used as a read-out for autophagy activity, with higher ratios indicating increased
147 autophagic flux.

148 Importantly, the basal autophagy level and compound sensitivity vary significantly depending
149 on the cell type and differentiation stage. We observed the most reproducible results when
150 performing microscopy experiments on epidermal root cells located at the beginning of the
151 differentiation zone (DZ, Fig. 3a).

152 Firstly, we performed an estimation of the optimal concentration and treatment duration. For
153 each compound a range of concentrations below the cytotoxicity level identified in the viability
154 assay was used to treat the TT reporter line only. The time-resolved changes in vacuolar
155 fluorescence were obtained using confocal microscopy. Confocal data were then automatically
156 processed by our designated ImageJ-based macro and R script (Figs. 3, Supplementary Fig. 2a,
157 Supplementary File 1). The optimal treatment conditions for each compound was then verified
158 using both control and reporter TT lines and the appropriate vehicle control (Fig. 3b). Figure
159 3b illustrates the effect on autophagy of a set of compounds whose treatments were previously
160 optimized to diminish cytotoxicity. The assay revealed that under the tested conditions several
161 compounds cause a significant change of the TT ratio compared to the vehicle treatment in the
162 reporter line (WT TT, Fig. 3b) but not in the control line (*atg5atg7* dKO TT, Fig. 3b).

163 The final fine-tuning of the treatment conditions is carried out using the TT assay as the last
164 step of phase four (feedback loop iii, Fig. 1a).

165 The TT assay in BY-2 cultures is less straightforward compared to Arabidopsis, due to the lack
166 of corresponding autophagy knockout background cell lines. Nevertheless, it still can be used
167 by combining TagRFP-mWasabi-ATG8 and TagRFP-mWasabi-NLS as a reporter and control
168 line for autophagic flux quantification, respectively (Fig. S2b).

169 **Phase three – verification of autophagic flux completion**

170 While the first two phases provide information about autophagy-dependent delivery of ATG8
171 to the lytic compartment, it still remains unclear whether the final step of autophagic flux, i.e.
172 cargo degradation, also takes place. The canonical assay to assess this is the GFP-ATG8
173 cleavage assay[22,23].

174 Arabidopsis plants expressing GFP-ATG8a in a WT or in autophagy-deficient background are
175 used as a reporter and control lines, respectively, for autophagic flux quantification (Fig. 1d).
176 Upon induction of autophagy, GFP-ATG8 is delivered to the vacuole at a higher rate, where it
177 is first cleaved off of the fusion protein by the lytic proteases, leading to transient accumulation
178 of the cleaved off GFP. Western blot analysis of the protein extracts allows estimation of a
179 ratio between the total and cleaved GFP in plant cells, thus revealing the relative level of
180 autophagic flux (Fig. 1d).

181 Importantly, tissue and organ-specific differences in the expression of 2x35S-driven GFP-
182 ATG8 and basal autophagic flux can considerably skew results. For example, protein extracts
183 from whole seedlings compared to the root differentiation zone of the same lines under the
184 same treatment conditions reveal significant differences in the read-out (Fig. 4a). We
185 established a designated protocol for the GFP-ATG8 cleavage assay for the Arabidopsis root
186 differentiation zone (Supplementary File 1) and obtained reproducible results consistent with
187 the results of the TT assay (Fig 4b, c; Fig 3b). Importantly, the combination of GFP-ATG8
188 cleavage assay results and the morphological and quantitative data from the TT assay may
189 indicate what step of the autophagy pathway is affected by the investigated compound
190 (feedback arrow ii, Fig. 1a). Interestingly, slightly greater concentrations of putative autophagy
191 modulators or longer incubation times were needed for efficient GFP-ATG8 cleavage assay,
192 compared to the TT assay. This might be caused by differences in the cells included into the
193 assay (epidermal layer for the TT assay *vs* all cell layers for the GFP-ATG8 cleavage assay) or
194 differences in the sensitivity of the methods. Alternatively, it might indicate that ATG8 fusion
195 hydrolysis does not occur immediately upon delivery of the autophagosomes to the lytic
196 compartment.

197 **Phase four – specificity check**

198 Autophagy is tightly integrated with endo- and exocytic pathways and the trafficking routes to
199 the vacuole[24–26]. Thus, it is probable that putative modulators of autophagy identified in the
200 previous phases of the screen might influence the endomembrane system and thus activate or

201 inhibit autophagy indirectly and have significant off-target effects, as it has been recently
202 shown for some of the known compounds[9,10].

203 To eliminate this possibility we designed the fourth phase of the screen where the effect of each
204 candidate compound on endomembrane compartments is tested *in planta* using a library of
205 fluorescent marker lines (Supplementary Table 3). The library comprises the minimal set
206 representing most crucial components of the endomembrane system including: endoplasmic
207 reticulum (ER), Golgi apparatus (GA), trans Golgi network (TGN), multi-vesicular bodies
208 (MVB), vacuole, mitochondria, peroxisomes, plasma membrane, endo- and exocytic pathways.

209 Firstly, each compound was tested on the set of the marker lines using the conditions optimized
210 in the second and third phases. If detectable morphological changes were observed for any of
211 the markers, a range of lower concentration of the compound and a range of different treatment
212 times were tested. This allowed to estimate the maximal possible concentration at which the
213 compound did not change the morphology of any endomembrane marker. Furthermore, the
214 identified concentration were then tested using the TT assay to assess its impact on autophagy
215 activity (feedback arrow iii, Fig. 1a).

216 Figure 5 provides an example of optimization for C12 that at conditions originally optimized
217 in phases two and three altered ER morphology. Thus, a gradient of C12 concentrations was
218 tested using an ER marker line (Fig. 5a). Concentrations of C12 at 60 µM and above were
219 causing significant ER stress, i.e. disrupted cisternae network and formation of swollen ER-
220 bodies (white arrows, Fig. 5a; Supplementary Video 1). C12 at 30 µM or less did not alter ER
221 morphology (Fig. 5a). Thus, C12 concentrations ranging from 7.5 µM to 30 µM were then
222 tested using the TT and GFPA-ATG8 cleavage assay and showed significant impact on
223 autophagic flux (Fig. 5b, c).

224 **Discussion**

225 Here we describe a novel robust pipeline designed for the fastest identification of chemical
226 compounds specifically modulating plant autophagy. Our approach significantly improves
227 reliability of the obtained hits and additionally provides data essential for further
228 characterization of the candidate drugs. One of the most important features of the new pipeline
229 is the combination of a high-throughput screen utilizing cell cultures with further verification
230 steps performed *in planta*. This approach simultaneously enables screening large numbers of
231 compounds and eliminates false positive candidates that for various reasons, although active in

232 cell cultures, do not have activity *in planta*, e.g. due differences in cell permeability, stability
233 in media used for cell culture and plant growth or cell-type-specific responses. Furthermore,
234 combining the use of *Nicotiana tabacum* cell cultures and *Arabidopsis thaliana* seedlings gives
235 a first estimation of potential conservation of the drug target in different plant species.
236 Interestingly, to our experience, the average concentration range of drugs applicable for BY-2
237 cells was significantly higher than the concentration range suitable for Arabidopsis plants,
238 indicating important differences between the two models. This observation is a useful starting
239 point for future drug screens utilizing either of the model systems. Notably, the absolute values
240 of the applicable concentration ranges have to be individually adjusted to a specific chemical
241 library, as the activity of compounds might vary due to purity, age, structural stability and
242 storage differences.

243 As further characterization of identified autophagy modulators is very costly and labour-
244 intensive[27,28], it is important to identify drugs that are specifically modulating autophagy under
245 physiological conditions. To achieve this, we designed a multi-faceted approach of the first
246 three phases that involves advanced fluorescent microscopy, biochemistry and cell and
247 molecular biology. It provides quantitative and morphological data on autophagy pathway
248 activity and is optimized to assess the effect of a drug on several key aspects of the pathway. It
249 not only ensures reliability of the conclusions about the drug effect on the plant autophagy, but
250 also provides an indication of the affected stage the pathway, e.g. phagophore formation, cargo
251 delivery or cargo degradation. While assays of the first three phases are focused on assessing
252 the drug effect on autophagy activity, the fourth phase puts the drug activity into a broader
253 context. Due to overwhelming complexity of the network, it is frequently overlooked that
254 autophagy is an integral part of the endomembrane trafficking system[26,29,30]. The assays in the
255 fourth phase help to identify treatment conditions under which the candidate drugs significantly
256 influence autophagy activity while not causing detectable aberrations in other components of
257 the trafficking machinery. Although informative, these assays do not provide a definite proof
258 of autophagy specificity of the drug. A more detailed estimation of potential off-targets of the
259 drug can be achieved via assessing its effect on the loss-of function mutants of the expected
260 target and predicted off-targets[31].

261 The pipeline described in this work is highly efficient in identifying specific regulators of plant
262 autophagy and fine tuning the treatment conditions for plants grown in laboratory conditions,
263 thus providing a very useful tool for fundamental plant autophagy research. Further

264 characterization of the identified drugs can be done either *via* conventional approaches for
265 target identification[27,32] or by directly testing the compounds on plants grown in soil. The first
266 approach will provide in depth mechanistic understanding of the drug activity - information
267 valuable for optimization of the drug specificity and potency and also for prediction of its
268 applicability for other species. The second approach might potentially streamline direct
269 application of the drug in the field, enabling the use of chemical transient modulators of plant
270 autophagy as potent regulators of crop fitness[1,4,33], thus benefiting modern agriculture.

271 **Methods**

272 *Genetic constructs*

273 Maps and sequences of all constructs used in this study can be found in Supplementary Table
274 1. Information about the primers used for cloning is available in Supplementary Table 2.

275 To generate the entry clone AM425, AtATG8a CDS was lifted from total cDNA of Arabidopsis
276 thaliana seedlings using primers AM18/AM19. The obtained attB-flanked amplicon was then
277 recombined with the Gateway™ pDONR™/Zeo vector (ThermoFisher) using Gateway™ BP
278 Clonase II enzyme mix (ThermoFisher).

279 Firefly luciferase (Fluc) and *Renilla* luciferase (Rluc) coding sequences were amplified using
280 primer pairs PB31/PB32 and PB33/PB34 and vectors pRD400 35S::Fluc and pRD400
281 35S::Rluc[34], respectively. The amplicons were inserted using KpnI/AscI restriction digestion
282 sites into a pMDC32 vector[35] that was previously modified to replace hyg resistance gene with
283 nptII sequence. The resulting binary Gateway™–based destination vectors were named AM
284 616 and AM 618 (Supplementary Table 1).

285 AM439 pMDC kan Fluc AtATG8a was obtained by recombining the entry clone AM425 (see
286 above) with AM616 pMDC kan Fluc using Gateway™ LR Clonase II enzyme mix
287 (ThermoFisher).

288 The synthetic sequence of attB-flanked SV40 NLS (Eurofins Scientific, Sweden) was
289 recombined with the Gateway™ pDONRTM/Zeo vector (ThermoFisher) using Gateway™ BP
290 Clonase II enzyme mix (ThermoFisher), producing entry clone CC3.

291 The CC3 entry clone was then recombined with the AM618 vector to produce an intermediate
292 clone containing the sequence of 2x35S::*Renilla*-NLS fusion::NosT. This sequence was lifted

293 using the 5'-phosphorylated primers CC1 and CC2. To generate the CC8 destination clone, the
294 amplicon was then blunt-end ligated into the AM439 destination clone linearized with the PmeI
295 restriction digestion enzyme (NEB).

296 The CC10 clone was obtained by introducing the stop codon between the Fluc and AtATG8a
297 utilizing The QuikChange® site-directed mutagenesis (Agilent) and primers CC7/CC8.

298 The sequence of TagRFP-mWasabi was lifted from the plasmid kindly provided by Zhou and
299 colleagues[12] using the primers PB15/PB16. The amplicon was inserted into pMDC32 or pMDC
300 kan to produce destination binary vectors, AM 613 and 614, respectively. The AM613 and 614
301 vectors were then recombined with the entry clone AM425 using Gateway™ LR Clonase II
302 enzyme mix (ThermoFisher) to produce AM 434 and AM435 clones, respectively.

303 *Plant material*

304 The description of stable transgenic lines used in this study is available in Table S3.

305 *Plant growth and transformation*

306 *Arabidopsis thaliana* seeds were surface sterilized using a bleach solution comprised of 10%
307 Klorin (Sweden) with 0.05% Tween-20 for at least 20 min, washed three times with sterile MQ
308 and plated on Murashige and Skoog (MS) plates: 0.5x MS including vitamins (M0222,
309 Duchefa), supplemented with 10 mM MES (M1503, Duchefa), 1% sucrose, 0.8 % Plant agar
310 (P1001, Duchefa), pH 5.8. Seeds on plates were then vernalized in the darkness at 4°C for 24-
311 48 h. After vernalization, plates were incubated vertically under long day growth conditions
312 (16 h of 150 µM light at 22°C, 8 h dark at 20°C).

313 For growth in sowing soil (2001, Hasselfors Garden) seeds were surface sterilized as described
314 above, vernalized in MQ water in Eppendorf tubes and then transferred directly into soil. Plants
315 in soil were grown under the long day conditions as described above.

316 For transformation, Arabidopsis plants were grown in soil for approximately 5 weeks, the first
317 inflorescence was clipped to stimulate production of auxiliary inflorescences. All genetic
318 constructs used for transformation were first introduced into *Agrobacterium tumefaciens* strain
319 GV3101[36]. The floral dip transformation was performed as previously described[37].
320 Transformants were selected on the 0.5x MS medium as described above supplemented with
321 400 µg/ml timentin (T0190, Duchefa), 250 µg/ml cefatoxime (C0111, Duchefa) and either 35

322 µg/ml hygromycin B (H0192, Duchefa) or 50 µg/ml kanamycin (K0126, Duchefa). Lines
323 showing a 3:1 segregation pattern in the T2 generation were used for establishing homozygous
324 T3 lines.

325 For testing potential inhibitors of autophagy, nitrogen starvation was induced in seedlings
326 grown *in situ* by incubating them in liquid –N MS medium: 0.5x MS basal salt micronutrient
327 solution (M0529, Sigma), 1% sucrose, 3mM $CaCl_2$, 1.5 mM $MgSO_4$, 1,25 mM KH_2PO_4, 5 mM
328 KCl, 0.8% Plant agar, pH 5.8. Seeds were germinated on normal MS medium as described
329 above. Seedlings were grown on vertically positioned plates under long day conditions for 4-5
330 d before being transferred into wells of 6-well tissue culture plates with 3 ml of –N MS medium.
331 The medium was gently pipetted on top of the roots to ensure their complete submersion.
332 Nitrogen starvation effect was clearly detectable after 18 h of treatment.

333 *BY-2 cell culture growth and transformation*

334 Tobacco BY-2 suspensions were subcultured under sterile conditions every 7-10 d using the
335 standard medium: 1x MS including vitamins (M0222, Duchefa), 0.02% KH_2PO_4, 0.2 mg/L
336 2,4-D, 3% Sucrose, pH 5.6. Erlenmeyer flasks with the cultures were incubated at 22°C in the
337 darkness, on a gyratory shaker at 120 rpm.

338 For our optimized transformation of BY-2 cells, overnight cultures of transgenic
339 *Agrobacterium tumefaciens* GV3101 were grown overnight at 28°C, 180 rpm, in 3 ml of LB
340 medium supplemented with 50 µg/ml rifampicin and 50 µg/ml kanamycin. Bacterial cells from
341 the overnight cultures were spun down for 15 min at 4 000 g, resuspended in 2 ml of BY-2
342 medium supplemented with 150 µM acetosyringone (D134406, Sigma) and incubated at 28°C,
343 120 rpm for one hour. The bacterial cells were then added to 4 ml of 4-d-old BY-2 culture to
344 the final OD_{600} of *Agrobacterium* = 0.375. The mixture was plated on plates with BY-2 medium
345 solidified with 0.8% agar. The plates were kept at 28°C for 48 h, after which the cells were
346 gently transferred on plates containing 400 µg/ml timentin (T0190, Duchefa), 250 µg/ml
347 cefatoxime (C0111, Duchefa) and either 40 µg/ml hygromycin B (H0192, Duchefa) or 50
348 µg/ml kanamycin (K0126, Duchefa). The first calli were typically visible after 2 weeks of
349 growth on the selection plates.

350 *Drug treatment of Arabidopsis seedling for microscopy*

351 For microscopy experiments, treatment of Arabidopsis seedlings with candidate compounds
352 was performed in 6-well tissue culture plates. Five-d-old Arabidopsis seedlings grown on
353 vertical plates were transferred into wells containing 3 ml of normal or –N MS medium
354 supplemented with a compound or the corresponding concertation of the vehicle (DMSO). The
355 seedlings were then submerged by gently pipetting the medium on the roots. The plates were
356 sealed with a strip of saran wrap and incubated in the growth cabinet under long day conditions
357 for the designated time. For microscopy the seedlings were mounted in the corresponding
358 treatment medium.

359 Prior to the viability assay, compound solubility was assessed in small volumes of MS medium
360 to exclude concentrations at which drug was not fully soluble. Viability assays were performed
361 using Zeiss AxioImager 2 epifluorescent microscope equipped with DIC (Nomarski) optics.
362 Images were acquired using ZEN blue software (Carl Zeiss).

363 *Drug treatment of BY-2 cells*

364 For the primary screen, 3-d-old BY-2 cell culture was pipetted into 96-well plates (140 µl/well),
365 using wide orifice tips. The plates were kept on an orbital shaker (4 mm) at 640 rpm, at 25°C
366 for 24 h to let cells recover from the mechanical stress. One µl of each compound taken from
367 the PMRP[19] and PMRA[20] libraries was pipetted into the plates with the BY-2 cells. One µM
368 AZD8055 (S1555, Selleckchem) and one mM BTH (32820, Sigma) were used as positive
369 controls for upregulation of autophagy, 1% DMSO was used as a negative control. The cells
370 were treated while shaking at 25°C, in the dark for 24 h, after which 50 µL of 4x Passive Lysis
371 Buffer (Dual Luciferase Assay kit, E1910, Promega) was added to all wells and the plates were
372 sealed and frozen at -80°C to rupture the cell walls. To measure the luciferase intensity values,
373 the plates were thawed at RT, vortexed for 2 min and spun down at 4 000g for 5 min. Ten µl
374 of each cell lysate were used for dual luciferase assay by applying 50 µL of freshly prepared
375 LARII and Stop&Glo reagents of the Dual Luciferase Assay kit (E1910, Promega). The
376 luciferase intensity values of firefly and *Renilla* luciferases were measured sequentially by
377 collecting one second of integrated chemiluminescence intensity (using gain 240) after a delay
378 of two seconds upon injection of each substrate (LARII and Stop&Glo respectively), using the
379 Synergy™ H4 Multi-Mode Microplate Reader (BioTek).

380 The obtained data was then analysed using RStudio (version 3.5.2). The compounds were
381 ranked according to their *Renilla* to firely luciferase intensity ratio and to their relative

382 luminescence unit (RLU) values for Rluc. The latter were used to infer the viability of the cells
383 and low values (below 150 000 RLU) were considered to correspond to cytotoxic effects from
384 the treatment. Rluc RLU values produced by dying cell cultures will vary depending on
385 detector sensitivity and therefore should be estimated prior to screening. Compounds inducing
386 a 2,5 to 3,33 fold change in *Renilla* to firefly luciferase ratio compared to the DMSO control
387 and Rluc RLU values above 150 000, were listed in the "loose selection group", while
388 compounds inducing more than 3,3 fold change in *Renilla* to firefly intensity ratios and Rluc
389 values above 200 000 RLU were listed in the "stringent selection group". Compounds inducing
390 a two-fold reduction in the *Renilla* to firely luciferase ratio and Rluc values above 150 000
391 RLU were selected as inhibitors.

392 Drug treatment of BY-2 cells for further analyses was performed in 6- or 24-well plate format
393 in 1-3.5 ml of 4-d-old BY-2 culture. After transfer into the plate and before the start of a
394 treatment, the cells were let to recover for 4-18 h. During treatment the plates were kept at
395 25°C, 120 rpm in the dark. For sampling the cells from each well were harvested onto a 50 µm
396 nylon mesh, frozen and ground in liquid nitrogen and resuspended in 1x passive lysis buffer
397 (Dual Luciferase Assay kit, E1910, Promega), using 2 volumes/mg of material. Ten µl of each
398 cell lysate were then transferred into another plate and used for dual Luciferase assay applying
399 quarter of the recommended volume of each reagent of the Dual Luciferase Assay kit (E1910,
400 Promega). The substrates were added by an automated pump of the FLUOstar Omega
401 Microplate Reader (BMG LABTECH) directly prior double orbital shaking at 100 rpm for 1 s
402 and then a 2 s reading interval for each well. The gain adjustment was estimated in a pilot
403 experiment using lysates of BY-2 cells treated with 1% DMSO, 500 nM AZD and 1 µM ConA.

404 *Tandem tag assay*

405 The detailed protocol for TT assay is described in Supplementary File 1.

406 *Western blot*

407 For the western blot analysis, Arabidopsis seedlings were grown on vertical plates as described
408 above. Briefly, seeds were sawn in two rows per plate and the seedlings were grown for 5-7 d
409 until the root became 4-5 cm long. For treatment with compounds, the plates were placed
410 horizontally and flooded with liquid 0.5x MS medium supplemented with the corresponding
411 drug. Treatments were performed in the growth cabinet under long day conditions. Upon the
412 completion of treatment, the excess liquid was poured out of the plates and the whole seedlings

were harvested and ground in liquid nitrogen. Alternatively, the differentiation zone of the root was excised using a scalpel blade, gently collected with the tweezers and briefly dried on a paper tissue to be then placed into a 1.5 ml Eppendorf and ground in liquid nitrogen with a plastic pestle. The powdered material was mixed 1:2 (m:V) with 2x Laemmli buffer[38], the mixture was thoroughly vortexed and boiled for 5 min at 95°C. Samples were spun down at 13 000 g for 10 min, 1-7.5 µl of the supernatant were loaded on precast gels (Bio-Rad). Proteins were transferred onto a PVDF membrane and blotted using 1:2000 a-GFP (Cat 632381, Clontech), 1:2000 a-actin (AS13 2640, Agrisera), 1:25 000 a-rabbit-HRP (AS09602, Agrisera), 1:8000 a–mouse-HRP (NA931, Amersham). The blots were developed using ECL Prime (Amersham) and GelDoc™ XR (Bio-Rad). The intensities of the bands were quantified using ImageJ or Image Studio Lite (LI-COR) software.

Statistical analysis and image preparation

Statistical analysis was performed using GraphPad Prism (GraphPad Software) unless otherwise stated. Figures were prepared using Adobe Photoshop and Illustrator CC (Adobe Inc.). Adjustments to brightness and contrast were applied equally to corresponding images within figures.

Acknowledgements

This project was supported by grants from Olle Engkvist Foundation (to PVB, EAM and SR), Carl Tryggers Foundation (to EAM), the Swedish Foundation for Strategic Research (to PVB), the Swedish Research Councils VR and Formas (to PVB), the Knut and Alice Wallenberg Foundation (to PVB) and by the research programme "Trees and Crops for the Future" at the Swedish University of Agricultural Sciences. Postdoctoral fellowship of AND was provided by the Natural Sciences and Engineering Research Council of Canada.

Author Contributions

AND performed most of the experiments for phases two through four and wrote a part of the manuscript. CC established and performed the primary screen in the phase one and established transgenic lines. KD helped establish the transgenic lines for the study. JAO contributed to designing the scripts for the automated vacuolar fluorescence intensity measurement. SBF contributed to the primary screen in the phase one. SR contributed to conceiving the project idea and the primary screen in the phase one. GRH assisted with

443 phase four experiments. PVB secured funding and contributed to conceiving the project
444 idea. EAM contributed to conceiving the project idea, supervised the project, performed
445 some experiments and wrote a part of the manuscript.

446 **Competing Interests statement**

447 The authors declare no conflicts of interest.

448 **Materials & Correspondence**

449 For material request and correspondence please contact Alyona Minina at
450 alena.minina@slu.se

451 **Data availability**

452 The data relevant to this article will be made available upon a personal request. Please note,
453 some of the information about identified modulators of plant autophagy will be made public
454 in upcoming publications.

455 **References**

456 1. Avin-Wittenberg, T. *et al.* Autophagy-related approaches for improving nutrient use
457 efficiency and crop yield protection. *J. Exp. Bot.* **69,** 1335–1353 (2018).

458 2. Minina, E. A., Bozhkov, P. V. & Hofius, D. Autophagy as initiator or executioner of
459 cell death. *Trends Plant Sci.* **19,** 692-697 (2014).

460 3. Minina, E. A., Moschou, P. N. & Bozhkov, P. V. Limited and digestive proteolysis:
461 crosstalk between evolutionary conserved pathways. *New Phytol.* **215,** 958-964 (2017).

462 4. Ustun, S. *et al.* Bacteria exploit autophagy for proteasome degradation and enhanced
463 virulence in plants. *Plant Cell* (2018). doi:10.1105/tpc.17.00815

464 5. Dagdas, Y. F. *et al.* An effector of the irish potato famine pathogen antagonizes a host
465 autophagy cargo receptor. *Elife* **5,** 1–23 (2016).

466 6. Ohsumi, Y. Historical landmarks of autophagy research. *Cell Res.* **24,** 9–23 (2014).

467 7. Klionsky, D. J. *et al.* Guidelines for the use and interpretation of assays for monitoring
468 autophagy (3rd edition). *Autophagy* **12**, 1-222 (2016).

469 8. Batoko, H., Dagdas, Y., Baluska, F. & Sirko, A. Understanding and exploiting
470 autophagy signaling in plants. *Essays Biochem.* **61,** 675–685 (2017).

471 9. Wu, Y. T. *et al.* Dual role of 3-methyladenine in modulation of autophagy via different
472 temporal patterns of inhibition on class I and III phosphoinositide 3-kinase. *J. Biol.*
473 *Chem.* **285,** 10850–10861 (2010).

474 10. Mauthe, M. *et al.* Chloroquine inhibits autophagic flux by decreasing autophagosome-
475 lysosome fusion. *Autophagy* **14,** 1435–1455 (2018).

476 11. Lorenz, M. C. & Heitman, J. TOR mutations confer rapamycin resistance by
477 preventing interaction with FKBP12-rapamycin. *J. Biol. Chem.* **270,** 27531–27537
478 (1995).

479 12. Zhou, C. *et al.* Monitoring autophagic flux by an improved tandem fluorescent-tagged
480 LC3 (mTagRFP- mWasabi-LC3) reveals that high-dose rapamycin impairs autophagic
481 flux in cancer cells. *Autophagy* **8,** 1215–1226 (2012).

482 13. Sormani, R. *et al.* Socchoromyces cerevisiae FKBP12 binds Arabidopsis thaliana TOR
483 and its expression in plants leads to rapamycin susceptibility. *BMC Plant Biol.* **7,** 1–8
484 (2007).

485 14. Xiong, Y. & Sheen, J. Rapamycin and Glucose-Target of Rapamycin (TOR) Protein
486 Signaling in Plants. *J. Biol. Chem.* **287,** 2836–2842 (2012).

487 15. Nagata, T., Nemoto, Y. & Hasezawa, S. Tobacco BY-2 cell line as the "HeLa" cell in
488 the cell biology of higher plants. *Int. Rev. Cyt.* **132**, 1–30 (1992).

489 16. Dong, P. *et al.* Expression profiling and functional analysis reveals that TOR is a key
490 player in regulating photosynthesis and phytohormone signaling pathways in
491 Arabidopsis. *Front. Plant Sci.* **6,** 1–15 (2015).

492 17. Yoshimoto, K. *et al.* Autophagy Negatively Regulates Cell Death by Controlling
493 NPR1-Dependent Salicylic Acid Signaling during Senescence and the Innate Immune
494 Response in Arabidopsis. *Plant Cell* **21,** 2914–2927 (2009).

495 18. Yoshimoto, K. Processing of ATG8s, Ubiquitin-Like Proteins, and Their
496 Deconjugation by ATG4s Are Essential for Plant Autophagy. *Plant Cell* **16,** 2967–

497 2983 (2004).

498 19. Robert, S. *et al.* Endosidin1 defines a compartment involved in endocytosis of the
499 brassinosteroid receptor BRI1 and the auxin transporters PIN2 and AUX1. *Proc. Natl.*
500 *Acad. Sci.* **105,** 8464–8469 (2008).

501 20. Drakakaki, G. *et al.* Clusters of bioactive compounds target dynamic endomembrane
502 networks in vivo. *Proc. Natl. Acad. Sci.* **108,** 17850–17855 (2011).

503 21. Di, L., Kerns, E. H., Chen, H. & Petusky, S. L. Development and application of an
504 automated solution stability assay for drug discovery. *J. Biomol. Screen.* **11,** 40–47
505 (2006).

506 22. Nair, U., Thumm, M., Klionsky, D. J. & Krick, R. GFP-Atg8 protease protection as a
507 tool to monitor autophagosome biogenesis. *Autophagy* **7,** 1546–1550 (2011).

508 23. Klionsky, D. J. *et al.* Guidelines for the use and interpretation of assays for monitoring
509 autophagy (3rd edition). *Autophagy* **12,** (2016).

510 24. Spitzer, C. *et al.* The Endosomal Protein CHARGED MULTIVESICULAR BODY
511 PROTEIN1 Regulates the Autophagic Turnover of Plastids in Arabidopsis. *Plant Cell*
512 **27,** 391–402 (2015).

513 25. Deretic, V., Jiang, S. & Dupont, N. Autophagy intersections with conventional and
514 unconventional secretion in tissue development, remodeling and inflammation. *Trends*
515 *Cell Biol.* **22,** 397–406 (2012).

516 26. Pečenková, T., Marković, V., Sabol, P., Kulich, I. & Zárský, V. Exocyst and
517 autophagy-related membrane trafficking in plants. *J. Exp. Bot.* **69,** 47–57 (2017).

518 27. Schenone, M., Wagner, B. K., Clemons, P. A. & Program, B. Target identification and
519 mechanism of action in chemical biology and drug discovery. *Nat. Chem. Biol.* **9,** 232–
520 240 (2017).

521 28. Hutson, P. H., Clark, J. A. & Cross, A. J. CNS Target Identification and Validation:
522 Avoiding the Valley of Death or Naive Optimism? *Annu. Rev. Pharmacol. Toxicol.* **57,**
523 171–187 (2017).

524 29. Ponpuak, M. *et al.* Secretory autophagy. *Curr. Opin. Cell Biol.* **35,** 106–116 (2015).

525 30. Søreng, K., Neufeld, T. P. & Simonsen, A. Membrane Trafficking in Autophagy. *Int.*
526 *Rev. Cell Mol. Biol.* **336,** (2017).

527 31. Robert, S., Raikhel, N. V. & Hicks, G. R. Powerful Partners: Arabidopsis and
528 Chemical Genomics. *Arab. B.* **7,** e0109 (2009).

529 32. Dejonghe, W. & Russinova, E. Target identification strategies in plant chemical
530 biology. *Front. Plant Sci.* **5,** 1–11 (2014).

531 33. Minina, E. A. *et al.* Transcriptional stimulation of rate-limiting components of the
532 autophagic pathway improves plant fitness. *J. Exp. Bot.* **69,** 1415–1432 (2018).

533 34. Eskelin, K., Hafren, A., Rantalainen, K. I. & Makinen, K. Potyviral VPg Enhances
534 Viral RNA Translation and Inhibits Reporter mRNA Translation In Planta. *J. Virol.*
535 **85,** 9210–9221 (2011).

536 35. Curtis, M. D. & Grossniklaus, U. A Gateway Cloning Vector Set for High-Throughput
537 Functional Analysis of Genes in Planta. *Plant Physiol.* **133,** 462–469 (2003).

538 36. Van Larebeke, N. *et al.* Large plasmid in Agrobacterium tumefaciens essential for
539 crown gall-inducing ability. *Nature* **252,** 169–170 (1974).

540 37. Clough, S. J. & Bent, A. F. Floral dip: A simplified method for Agrobacterium-
541 mediated transformation of Arabidopsis thaliana. *Plant J.* **16,** 735–743 (1998).

542 38. Laemmli, U. K. Cleavage of Structural Proteins during the Assembly of the Head of
543 Bacteriophage T4. *Nature* **227,** 680–685 (1970).

544 39. Thompson, A. R. Autophagic Nutrient Recycling in Arabidopsis Directed by the
545 ATG8 and ATG12 Conjugation Pathways. *Plant Physiol.* **138,** 2097–2110 (2005).

546 40. Nelson, B. K., Cai, X. & Nebenführ, A. A multicolored set of in vivo organelle
547 markers for co-localization studies in Arabidopsis and other plants. *Plant J.* **51,** 1126–
548 1136 (2007).

549 41. Grebe, M. *et al.* Arabidopsis Sterol Endocytosis Involves Actin-Mediated Trafficking
550 via ARA6-Positive Early Endosomes. *Curr. Biol.* **13,** 1378–1387 (2003).

551 42. Dettmer, J. Vacuolar H+-ATPase Activity Is Required for Endocytic and Secretory
552 Trafficking in Arabidopsis. *Plant Cell* **18,** 715–730 (2006).

553 43. Drakakaki, G. *et al.* Isolation and proteomic analysis of the SYP61 compartment
554 reveal its role in exocytic trafficking in Arabidopsis. *Cell Res.* **22,** 413–424 (2012).

555 44. Chow, C.-M., Neto, H., Foucart, C. & Moore, I. Rab-A2 and Rab-A3 GTPases Define
556 a trans-Golgi Endosomal Membrane Domain in Arabidopsis That Contributes
557 Substantially to the Cell Plate. *Plant Cell* **20,** 101–123 (2008).

558 45. Boutté, Y. *et al.* Endocytosis restricts Arabidopsis KNOLLE syntaxin to the cell
559 division plane during late cytokinesis. *EMBO J.* **29,** 546–558 (2010).

560 46. Geldner, N. *et al.* Rapid, combinatorial analysis of membrane compartments in intact
561 plants with a multicolor marker set. *Plant J.* **59,** 169–178 (2009).

562 47. Nodzyński, T. *et al.* Enquiry into the Topology of Plasma Membrane-Localized PIN
563 Auxin Transport Components. *Mol. Plant* **9,** 1504–1519 (2016).

564 48. Saito, C. *et al.* A complex and mobile structure forms a distinct subregion within the
565 continuous vacuolar membrane in young cotyledons of Arabidopsis. *Plant J.* **29,** 245–
566 255 (2002).

567 49. Thordal-Christensen, H., Ueda, T., Nielsen, M. E., Feechan, A. & Bohlenius, H.
568 Arabidopsis ARF-GTP exchange factor, GNOM, mediates transport required for
569 innate immunity and focal accumulation of syntaxin PEN1. *Proc. Natl. Acad. Sci.* **109,**
570 11443–11448 (2012).

571 50. Ito, E. *et al.* Dynamic behavior of clathrin in Arabidopsis thaliana unveiled by live
572 imaging. *Plant J.* **69,** 204–216 (2012).

573 51. Zheng, H., Kunst, L., Hawes, C. & Moore, I. A GFP-based assay reveals a role for
574 RHD3 in transport between the endoplasmic reticulum and Golgi apparatus. *Plant J.*
575 **37,** 398–414 (2004).

576 52. Munch, D. *et al.* Retromer Contributes to Immunity-Associated Cell Death in
577 Arabidopsis. *Plant Cell* **27,** 463–479 (2015).

578 **Figures**

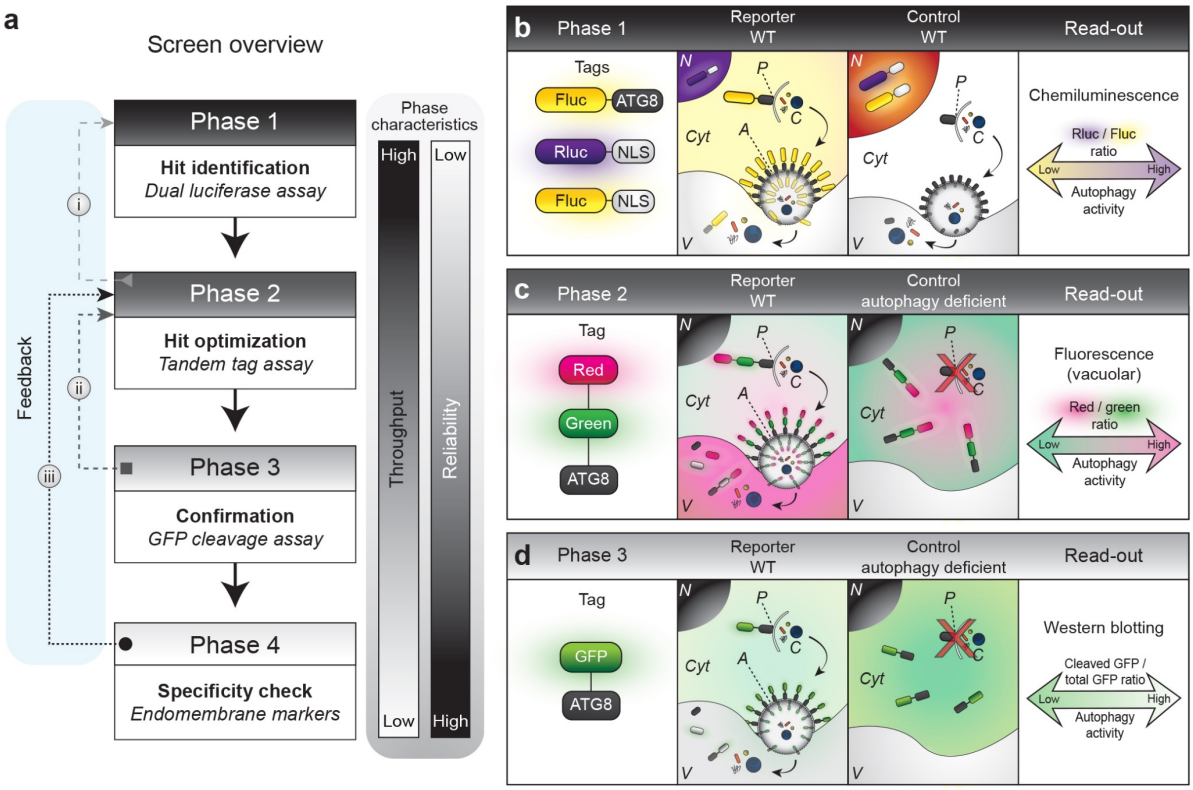

579

580 **Fig. 1: Multiphasic screen for autophagy-modulating compounds.**
581 **a**, The screen comprises four interconnected phases that allow to identify the best candidate
582 compounds and verify their specificity. The first phase is performed in a high–throughput
583 mode, testing a library of drugs on cells expressing reporter and control constructs. The assay
584 is performed in lysates of treated cells and can provide quantitative end-point read out. The
585 assay of the second phase is performed *in planta* and has lower throughput as it employs
586 advanced microscopy. It provides real-time quantitative read-out of autophagy activity and
587 morphological data. While the read-out in the first two phases is based on delivery of
588 autophagosomal membranes to the lytic vacuole, the third phase, quantifies degradation of
589 autophagic cargo, i.e. completion of the autophagic flux. Phase four is an essential step of the
590 screen that verifies specificity of the drug effect to autophagy *in planta* using transgenic
591 endomembrane marker lines. Importantly, results obtained in each phase are used for
592 optimization of the previous steps: optimization of drug concentration range for future screens
593 (dashed arrow, i); estimation of efficacy and timing of cargo delivery versus its degradation
594 (dashed arrow, ii); optimization of drug concentration range for autophagy-specific drug effect
595 (dashed arrow, iii). **b,** In the first phase a high throughput screen of drugs modulating
596 autophagy is performed using the dual luciferase assay. **b,** Reporter: wild-type (WT) tobacco
597 BY-2 cells co-expressing firefly luciferase (Fluc) fused to ATG8 and *Renilla* luciferase (Rluc)
598 fused to nuclear localization signal (NLS). Upon activation of autophagy, Fluc-ATG8
599 incorporates into autophagosome membranes and is delivered to the vacuole where Fluc
600 activity is lost, while Rluc-NLS levels are unaffected. **b,** Control: WT BY-2 cells co-expressing
601 Fluc-NLS and Rluc-NLS, which are unaffected upon autophagy upregulation. **b,** The read-out
602 for phase one is the ratio between chemiluminescence intensities of Rluc and Fluc substrates
603 measured in cell lysates. **c,** In the second phase, delivery of ATG8 to the lytic vacuole is
604 assessed using confocal microscopy. For this the tandem tag (TT) of red (TagRFP) and green

605 (mWasabi) fluorescent proteins fused to ATG8 is expressed in a WT background (reporter) or
606 in an autophagy-deficient *atg5atg7* double knockout (dKO) background (control). Upon
607 activation of autophagy, the TT-ATG8 is delivered to the vacuole in the reporter line (**c**), where
608 green fluorescence is quenched by the acidic pH, while red fluorescence persists. The ratio
609 between red and green fluorescence intensities in the vacuole are representative of
610 autophagosome delivery to the lytic compartment. **d**, In phase three the canonical GFP-
611 cleavage western blot assay is implemented to assess completion of autophagic flux. For the
612 assay, GFP-ATG8 is expressed in either a WT plants (reporter) or in *atg5* KO background
613 (control). Upon activation of autophagy in the reporter line, the GFP-ATG8 fusion is delivered
614 to the vacuole and cleaved. Thus the ratio of cleaved *vs* total GFP provides the read-out for
615 autophagy activity. Abbreviations, A = autophagosome; C = cargo; Cyt = cytoplasm; N =
616 nucleus; P = phagophore; V = vacuole.
617

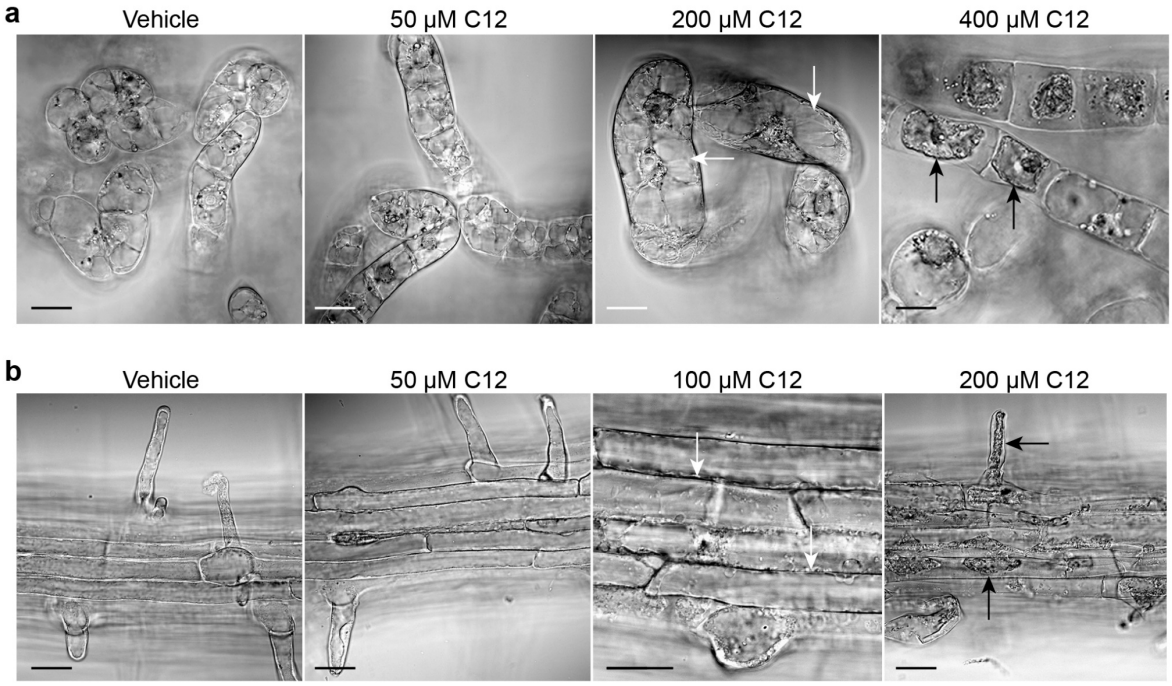

618

619 **Fig. 2: Phase two — viability testing.**
620 **a,** Tobacco BY-2 cell cultures and **b,** roots of 5-d-old Arabidopsis seedlings exposed to a
621 concentration gradient of compound 12 (C12) dissolved in 1% DMSO (vehicle) for 4 h.
622 Viability is assessed at 0, 2, 4 and 6 h using DIC light microscopy. Swollen (white arrows, **a**)
623 and collapsed protoplasts (black arrows, **a**) in BY-2 cells at 200 and 400 µM concentrations,
624 respectively. Arabidopsis roots with wrinkled (white arrows, **b**) or collapsed protoplasts (black
625 arrows, **b**) at 100 and 200 µM concentrations, respectively. Scale bars, 20 µm (**a-b**).
626

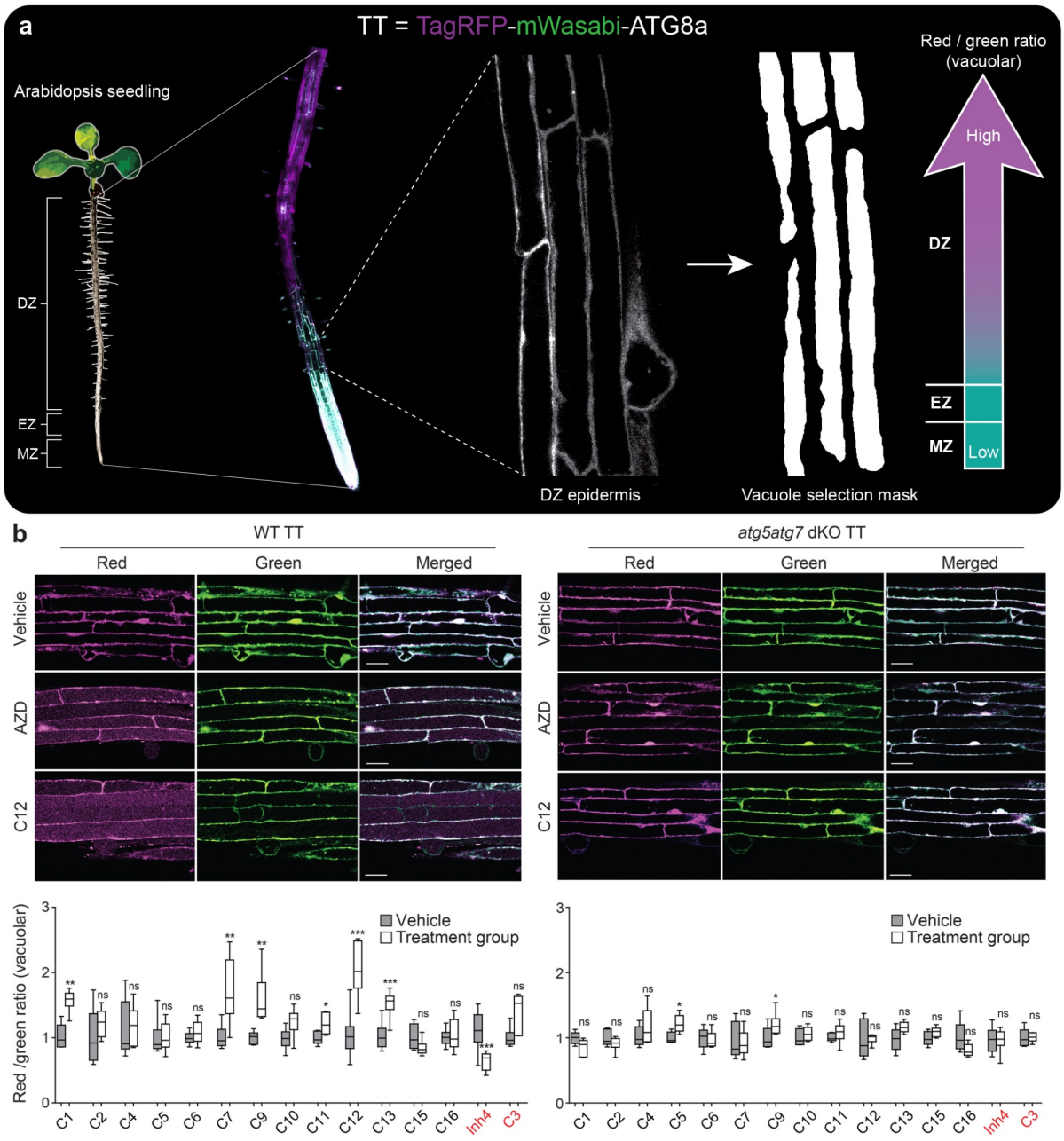

Fig. 3: Phase two continued — hit verification and optimization *in vivo*.
a, Roots of Arabidopsis seedlings (5-d-old) expressing the Tandem Tag (TT; TagRFP-mWasabi-ATG8a) are utilized for drug hit optimization. The epidermal layer at the beginning of the root differentiation zone (DZ), located above the elongation and meristematic zones (EZ and MZ, respectively) is scanned via confocal microscopy. Images are then processed by our script to automatically quantify red and green fluorescence intensities in the vacuoles and perform statistical analysis of red to green ratios *vs* time or concentration. **b,** The TT vector is expressed in wildtype (WT) and *atg5atg7* double knockout (dKO) Arabidopsis lines to determine the effects of each compound (C1-C16, Inh4) on autophagic flux. Treatments represented by red text (Inh4 and C3) are performed on seedlings exposed to nitrogen starvation for 24 h. Statistical information: n ≥ 6; ***$P < 0.005$; **$P < 0.01$; *$P < 0.05$; ns = non-significant (Student's t-test); error bars represent SEM. Scale bars, 15 µm (**b**).

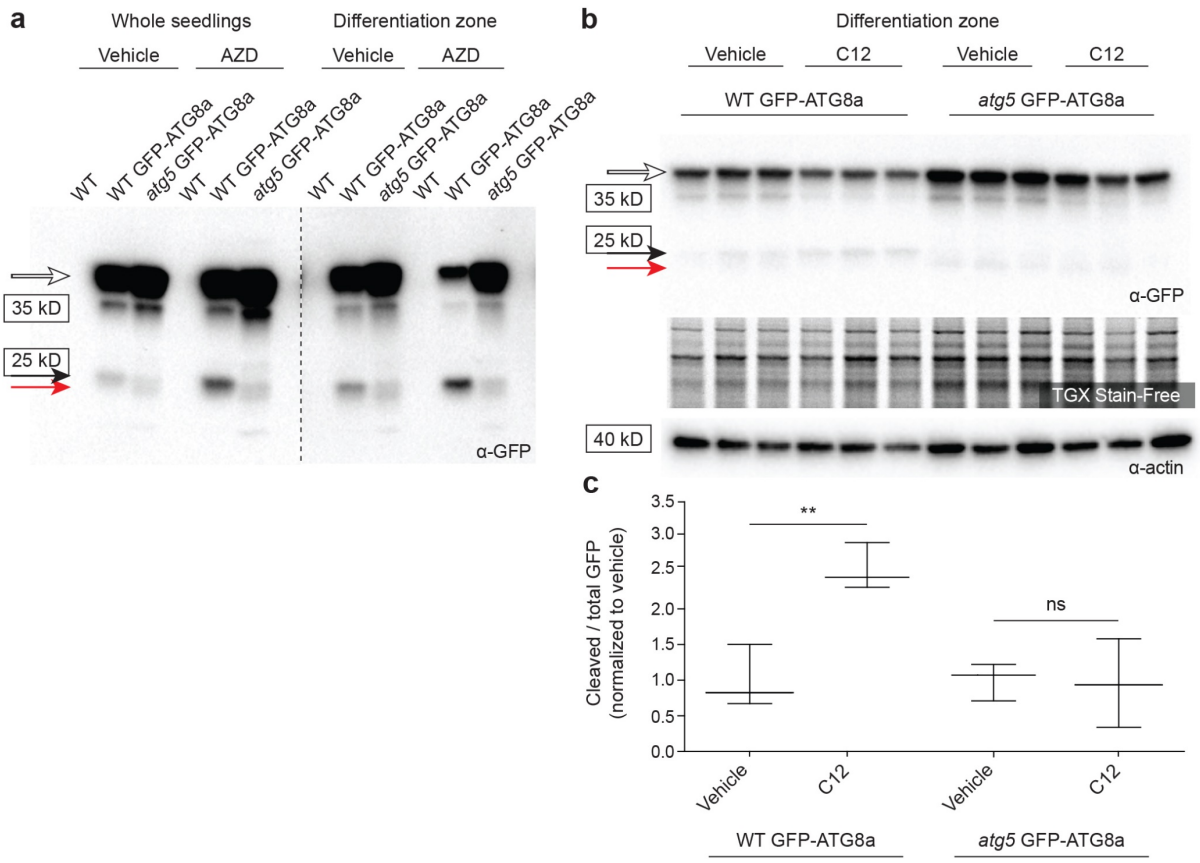

Fig. 4: Phase three — validation of autophagic flux completion.
a, Green fluorescent protein (GFP) cleavage assay for Arabidopsis whole seedling and root differentiation zone protein extracts from the following lines: Wild-type (WT), GFP-ATG8a expressed in WT (WT GFP-ATG8) and *atg5* KO (*atg5* GFP-ATG8a). Treatments were applied for 6 h prior to protein extraction and included a vehicle control (1% DMSO) and 0.5 µM AZD8055 (AZD). **b,** Immunoblotting with α-GFP of differentiation zone protein extracts from WT GFP-ATG8a and *atg5* GFP-ATG8a lines (three independent replicates per treatment and genetic background) treated with 1% DMSO (vehicle) or 30 µM of compound 12 (C12) for 4h. Bio-Rad TGX Stain-Free gels and α-actin are utilized as loading controls. **(a, b)** GFP-ATG8a fusion band (white arrow); Cleaved GFP (black arrow); lower molecular weight band (red arrow). Dashed line indicates membrane splicing. **c,** Cleaved versus total GFP ratios comparing vehicle and 30 µM C12 treatment in WT GFP ATG8a and *atg5* GFP-ATG8a lines. Statistical information: n = 3; $^{**}P < 0.01$; ns = non-significant (Student's t-test); error bars represent SEM.

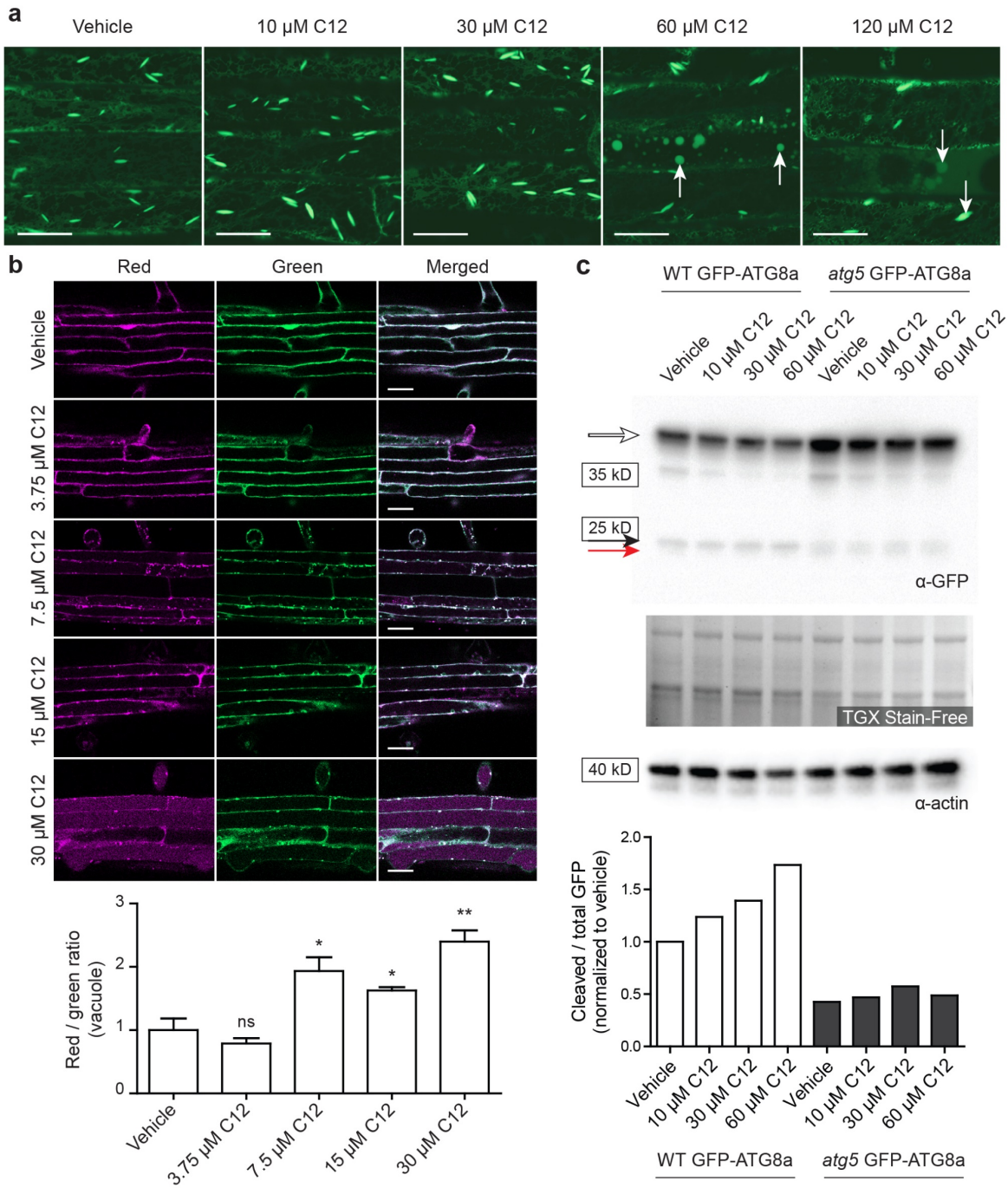

Fig. 5: Phase four – identification of autophagy-specific compounds and conditions. **a,** HDEL-GFP Arabidopsis seedlings exposed to a gradient of compound 12 (C12) concentrations to assess its phenotypic effects on the endoplasmic reticulum (ER). Swollen ER bodies (white arrows) and disrupted ER networks occur at higher concentrations (60 and 120 µM). **b**, Tandem tag (TagRFP-mWasabi-ATG8a) reporter lines treated with a range of C12 concentrations. **c,** The GFP-cleavage assay for a gradient of C12 treatments. Western blot detection of GFP in protein extracts prepared differentiation zone of WT GFP-ATG8a and *atg5* GFP-ATG8a lines. Bio-Rad TGX Stain-Free gels and α-actin immunoprobing are used as loading controls. GFP-ATG8a fusion band (white arrow); cleaved GFP (black arrow); lower molecular weight band (red arrow). Scale bars, 15 µm (**a**), 20 µm (**b**). Statistical information (**b**): n = 3; $^{**}P < 0.01$; $^{*}P < 0.05$; ns = non-significant (Student's t-test); error bars represent SEM.

670 **Supplementary information**

671 Supplementary Figs. 1-2,
672 Supplementary Video 1,
673 Supplementary File 1,
674 Supplementary Tables 1-3
675

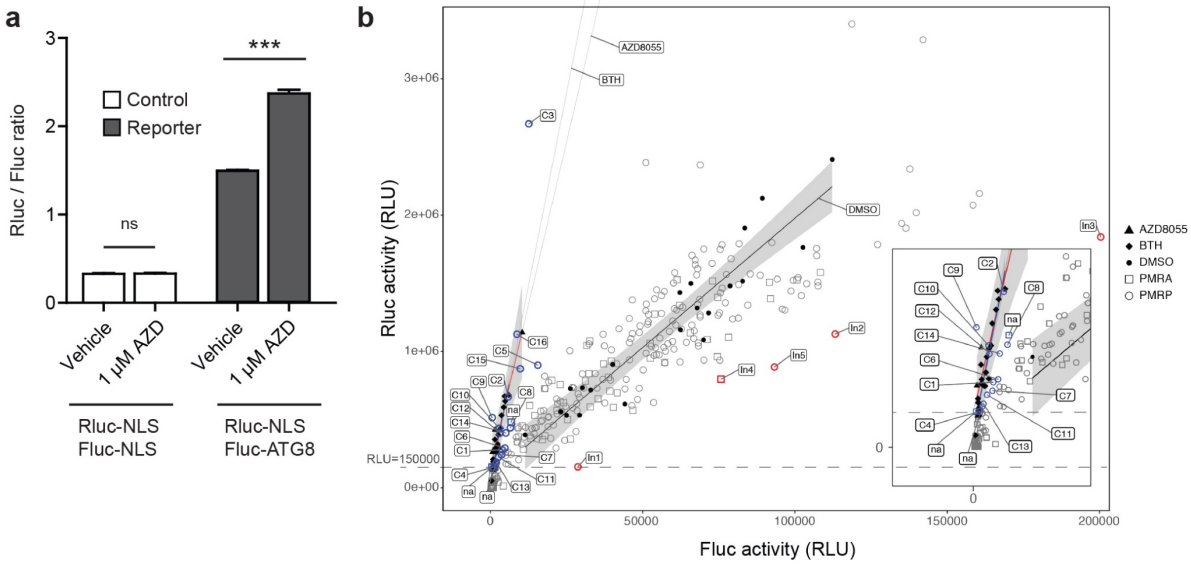

676

677 **Supplementary Fig. 1: BY-2 dual luciferase reporter verification and hit identification.**
678 **a,** Dual luciferase assay validation in tobacco BY-2 cell cultures. Control cell lines co-
679 expressing *Renilla* luciferase (Rluc) and firefly luciferase (Fluc) fused to Nuclear Localization
680 Signal (NLS) and reporter lines co-expressing Rluc-NLS and Fluc fused to ATG8. Upon
681 activation of autophagy by AZD8055 (AZD) the ratio of Rluc/Fluc increases in the reporter
682 but not in the control. Statistical information: n = 3; ***$P < 0.0001$; ns = non-significant
683 (Student's t-test); error bars represent SEM. **b,** Hit identification using the tobacco BY-2
684 reporter line. A preselected library of 364 compounds reveals several strong inhibitors (> 2-
685 fold decrease in Rluc/Fluc ratio, highlighted in red) and enhancers (> 3.3 fold increase in
686 Rluc/Fluc ratio, highlighted in blue). Enhancers with relative luminescence unit (RLU) values
687 below 150000 were considered potentially cytotoxic and were excluded from further
688 characterization. Lines and shaded areas represent the linear regressions and 95% confidence
689 intervals each control treatment: DMSO (black), BTH (blue) and AZD8055 (red).

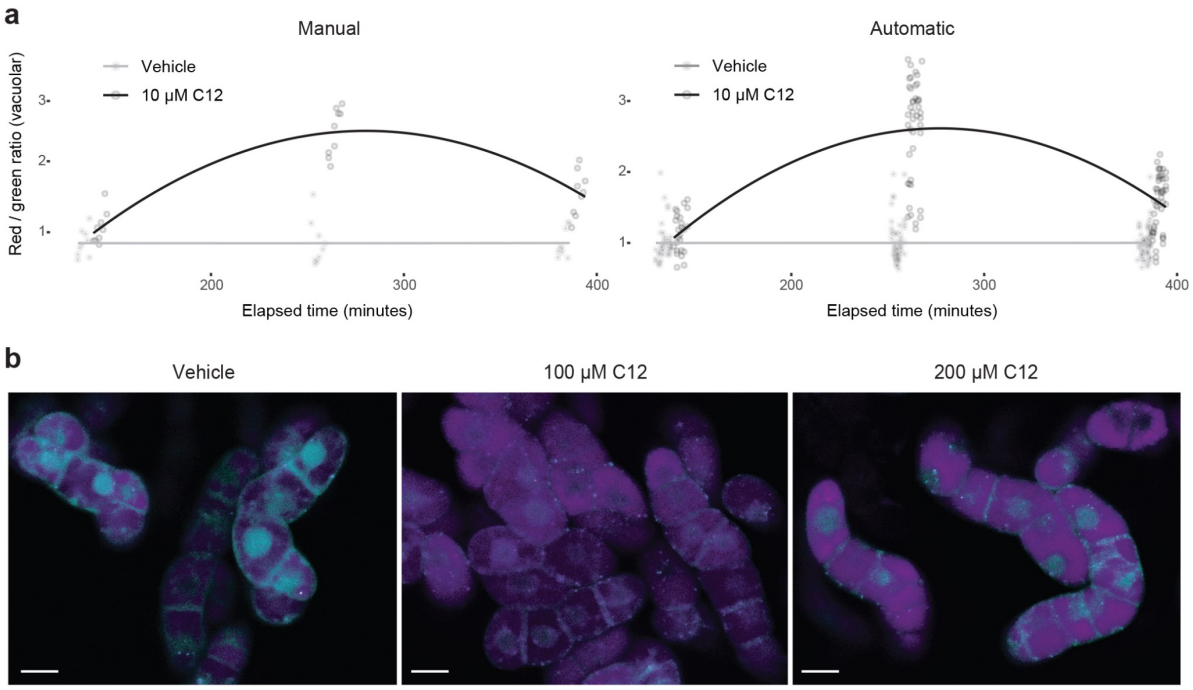

Supplementary Fig. 2: Tandem tag assay.
a, Comparison of manual and automatic quantification of vacuolar red to green fluorescence intensities ratios in *Arabidopsis* seedlings expressing tandem tag (TagRFP-mWasabi-ATG8) and treated with 10 µM compound 12 (C12) or vehicle (1% DMSO). **b,** An example of tandem tag detection in tobacco BY-2 cell cultures treated with the vehicle (1% DMSO), 100 µM C12 and 200 µM C12 for 4 h. Scale bars, 20 µM (**b**).

Supplementary Video 1: Phase four examples.
a, Timeseries and Z-stacks (**b**) of Arabidopsis seedling expressing the ER-marker HDEL-GFP. (**a**, **b**) Root differentiation zone epidermal cells from vehicle (1% DMSO), 10 µM compound 12 (C12) and 60 µM C12 treatment groups. Timeseries acquisition time: 2 minutes. Click on individual videos to start and stop playback.

713 **Supplementary Table 1. Constructs used in this study.**

Code	Construct Name	Gene Insert	BR	PR
Reporters for the dual luciferase assay				
AM 425	pDONR Zeo AtATG8a CDS	AtATG8a CDS	zeo	-
AM 616	pMDC kan Fluc	2x35S::Fluc::Gateway cassette::NosT	kan	kan
AM 618	pMDC kan Rluc	2x35S::Rluc::Gateway cassette::NosT	kan	kan
AM 439	pMDC kan Fluc AtATG8a	2x35S::Fluc::AtATG8a CDS::NosT	kan	kan
CC3	pDONR Zeo SV40 NLS	SV40 NLS	zeo	-
CC 8	dLuc reporter 2d generation	2x35S::Fluc-AtATG8a::NosT/2x35S::Rluc-NLS::NosT	kan	hyg
CC10	dLuc control 2d generation	2x35S::Fluc-STOP-AtATG8a::NosT/2x35S::Rluc-NLS::NosT	kan	hyg
Reporters for the tandem tag assay				
AM 613	pMDC hyg TT vector	2x35S::TagRFP-mWasabi::Gateway cassette::NosT	kan	hyg
AM 614	pMDC kan TT vector	2x35S::TagRFP-mWasabi::Gateway cassette::NosT	kan	kan
AM 434	pMDC hyg TT AtATG8a	2x35S::TagRFP-mWasabi-AtATG8a::NosT	kan	hyg
AM 435	pMDC kan TT AtATG8a	2x35S::TagRFP-mWasabi-AtATG8a::NosT	kan	kan

714 Abbreviations: BR = Bacterial resistance marker; dLuc = dual luciferase; Fluc = firefly
715 luciferase; Rluc = *Renilla* luciferase; PR = Plant resistance marker; hyg = hygromycin; kan =
716 kanamycin; zeo = zeomycin.
717
718
719
720
721
722
723
724
725
726
727
728
729
730
731
732
733
734
735
736
737
738
739
740
741
742
743
744
745
746

747 **Supplementary Table 2. Primers used in this study.**

Code	Primer name	5'->3' sequence	Purpose
Cloning			
AM18	attB1 AtATG8a	GGGG ACA AGT TTG TAC AAA AAA GCA GGC T TG ATG GCT AAG AGT TCC TTC AAG A	pDONR Zeo AtATG8a CDS
AM19	attB2 AtATG8a	GGGG AC CAC TTT GTA CAA GAA AGC TGG GT TCA AGC AAC GGT AAG AGA TCC A	pDONR Zeo AtATG8a CDS
PB 15	KpnI-Tag RFP-Fw	TTG GTA CCA TGA GCG AGC TGA TTA AGG AGA ACA	generating TT vectors
PB 16	AscI-mWassabi-Re	TTG GCG CGC CCT TGT ACA GCT CGT CCA TGC CGT	generating TT vectors
PB 31	F.Lucifer Fw	TTGGTACCATGGAAGACGCCAAAAACATAAAGA	generating pMDC Fluc vectors
PB 32	F.Lucifer Re	TTGGCGCGCCCAATTTGGACTTTCCGCCCTTCTT	generating pMDC Fluc vectors
PB 33	R.Lucifer Fw	TTGGTACCATGACTTCGAAAGTTTATGATCCA	generating pMDC Rluc vectors
PB 34	R.Lucifer Re	TTGGCGCGCCTTGTTCATTTTTGAGAACTCGCTCA	generating pMDC Rluc vectors
CC1	Nos T PHO	5'PHO-ACTCTAATCATAAAAACCCATCTCATAAATAACG-3'	generating pMDC kan Fluc-AtATG8a-Rluc-Gateway cassette
CC2	35S PHO	5'PHO-CCTGCAGGTCAACATGGTGGA-3'	generating pMDC kan Fluc-AtATG8a-Rluc-Gateway cassette
CC8	FlucSTOPattB FW	tcaagcctgctttttgtacaattatcattgatagcttggcgcgcccaatttggac	generating pMDC kan Fluc-STOP-AtATG8a-Rluc-NLS
CC7	FlucSTOPattB RV	gtccaaattgggcgcgccaagctatcaatgataattgtacaaaaaagcaggcttga	generating pMDC kan Fluc-STOP-AtATG8a-Rluc-NLS
Genotyping			
AM1	ATG5-1 Fw	ATACACTTTAGAGGATATCC	genotyping atg5-1 KO
AM2	ATG5-1 Re	CTGTCTTAACTTGTCCAGCCA	genotyping atg5-1 KO
AM 579	LB1 (SAIL)	GCC TTT TCA GAA ATG GAT AAA TAG CC	genotyping atg5-1 and 7-2 KO
AM12	ATG7-2 Fw	tct gct gtc gat tta aac tt	genotyping atg7-2 KO
AM13	ATG7-2 Re	AGGTGCAACCACGTCGTTGCA	genotyping atg7-2 KO
CC11	Fluc_gen1 fw	CCTCATAAAGGCCAAGAAGG	FlucAtATG8a Rluc BY-2 and Arabidopsis genotyping
CC10	Rluc_gen1 fw	ccaggattcttttccaatgc	FlucAtATG8a Rluc BY-2 and Arabidopsis genotyping
CC12	nos_term_gen1 rv	AAGGAATTATCGAACCACTTTG	FlucAtATG8a Rluc BY-2 and Arabidopsis genotyping
CC9	Cmr/CAT_gen1 rv	atcaccagctcaccgtcttt	FlucAtATG8a Rluc BY-2 and Arabidopsis genotyping

748 Abbreviations: TT = tandem tag; KO = knockout; BY-2 = bright yellow 2; Fluc = firefly
749 luciferase; Rluc = *Renilla* luciferase; 5'PHO = modification (5'-phosphorilated for blunt end
750 ligation).

751

752

753

754

755

756 **Supplementary Table 3. Stable transgenic lines used in this study.**

Line	Transgene	BG	Acc	Gen	HO	PR	Origin
Tobacco BY-2 Cell Lines							
dLuc reporter	2x35S::Fluc-AtATG8a::NosT/2x35S::Rluc-NLS::NosT	WT	N/A	N/A	N/A	hyg	This study
dLuc control	2x35S::Fluc-STOP-AtATG8a::NosT/2x35S::Rluc-NLS::NosT	WT	N/A	N/A	N/A	hyg	This study
TT reporter	2x35S::TagRFP-mWasabi-AtATG8a::NosT	WT	N/A	N/A	N/A	kan	This study
TT control	2x35S::TagRFP-mWasabi::NosT	WT	N/A	N/A	N/A	kan	This study
Arabidopsis thaliana lines							
TT reporter	2x35S::TagRFP-mWasabi-AtATG8a::NosT	WT	Col-0	T3	HO	hyg	This study
TT control	2x35S::TagRFP-mWasabi-AtATG8a::NosT	atg5-1/atg7-2	Col-0	T3	HO	hyg	This study
GFP-ATG8a reporter	2x35S::GFP-AtATG8a	WT	Col-0	N/A	HO	basta	(Thompson et al.)[39]
GFP-ATG8a control	2x35S::GFP-AtATG8a	atg5-1	Col-0	F5	HO	basta	(Minina et al.)[33]
35S GFP-HDEL	2x35S::GFP-HDEL	WT	Col-0	N/A	HO	kan	(Nelson & Nebenfuhr)[40]
35S MT-YFP	2x35S::MT-YFP	WT	Col-0	N/A	HO	kan	(Nelson & Nebenfuhr)[40]
35S::NAG1-eGFP	35S::NAG1-eGFP	WT	Col-0	T3	HO	N/A	(Grebe et al.)[41]
VHAa1::VHAa1-GFP	VHAa1::VHAa1-GFP5(S65T)	WT	Col-0	N/A	HO	kan	(Dettmer et al.)[42]
SYP61-GFP	35S::SYP61-GFP	WT	Col-0	N/A	HO	N/A	(Drakakaki et al.)[43]
Rab A2a-YFP	Rab-A2a::YFP-Rab-A2a	WT	Col-0	N/A	HO	N/A	(Chow et al.)[44]
Knolle-GFP	KNOLLE::GFP-KNOLLE	WT	Ler	N/A	HO	N/A	(Boutte et al.)[45]
VAMP711-Cherry	N/A	WT	N/A	N/A	HO	N/A	(Geldner et al.)[46]
SYP22::SYP22-YFP	SYP22::SYP22-YFP	WT	Col-0	N/A	HO	N/A	(Nodzynsky et al.)[47]
gammaTIP-GFP	35S::gammaTIP-GFP	WT	Col-0	N/A	HO	kan	(Saito et al.)[48]
PEN1-GFP in pen1-1 KO background	35S::GFP-PEN1	pen1 KO	Col-0	N/A	HO	N/A	(Nielssen et al.)[49]
DRP1a-GFP	35S::DRP1a-GFP	WT	Col-0	N/A	HO	kan	(Fujimoto et al.)[50]
CLC-GFP	CLC2::CLC-GFP	WT	N/A	N/A	HO	N/A	(Ito et al.)[50]
secGFP	35S::Sec-GFP	WT	Col-0	N/A	HO	hyg	(Zheng et al.)[51]
GFP-VSP35B in vps35b-2 KO	VPS35B::VPS35B-GFP	vps35b KO	Col-0	N/A	HO	kan	(Munch et al.)[52]

757 Abbreviations: BY-2 = bright yellow 2; TT = tandem tag; Fluc = firefly luciferase; Rluc =
758 *Renilla* luciferase; dLuc = dual luciferase; BG = background; Acc = Accession; Gen =
759 Generation; HO = Homozygous; PR = Plant resistance marker; WT = wildtype; KO =
760 knockout; N/A = not available.